Electronic Spectroscopy of UO_2Cl_2 Isolated in Solid Ar†

Jin Jin, Raj Gondalia, and Michael C. Heaven*

Department of Chemistry, Emory University, Atlanta, Georgia 30322

Received: June 3, 2009; Revised Manuscript Received: July 10, 2009

Laser-induced fluorescence spectra have been recorded for uranyl chloride isolated in a solid Ar matrix. Pulsed excitation was examined using a XeCl excimer laser (308 nm) and a dye laser operating in the 19 500−27 500 cm^{-1} range. Several absorption and emission band systems were observed. The emission spectra were characterized by a nearly harmonic vibrational progression with a frequency of 840 cm^{-1} starting at 20 323 cm^{-1}. The electronic absorption spectra were dominated by five harmonic vibrational progressions with frequencies of approximately 710 cm^{-1}. Comparisons with theoretical calculations indicate that all of the transitions observed were associated with the UO2+2 subunit. They involved the promotion of an electron from a bonding orbital to the metal-centered $5f_\delta$ and $5f_\phi$ orbitals. Band origins and vibrational constants for five excited states were obtained. Fluorescence was observed from the lowest-energy excited state alone, regardless of the excitation wavelength. The decay curve was found to be biexponential, with characteristic decay lifetimes of 50 and 260 μs.

Introduction

The uranyl ion (UO2+2) is a species of central importance in the chemistry of uranium. Consequently, it has been the subject of numerous experimental and theoretical investigations.[1−16] Uranyl has very distinctive optical properties. Spectra for the isolated ion have yet to be recorded, but the long history of spectroscopic work on uranyl salts has been eloquently summarized by Zhang and Pitzer[1] and Denning.[6] Some of the most detailed and informative spectroscopic studies have been carried out for crystals of $Cs_2UO_2Cl_4$ and $CsUO_2(NO_3)_3$ under low temperature conditions.[6] The spectra for these compounds can be understood in terms of a linear UO2+2 subunit that is weakly perturbed by the surrounding ligands. The HOMO for uranyl is a σ_u bonding orbital that is primarily composed of the O $2p_\sigma$ and U $5f_\sigma$ orbitals. The LUMOs are metal-centered $5f_\delta$ and $5f_\phi$ orbitals. Therefore the lowest-energy electronic transitions are ascribed to $\sigma_u^2 \rightarrow \sigma_u\delta_u$ and $\sigma_u^2 \rightarrow \sigma_u\phi_u$ promotions. For the linear ion, these transitions are electric-dipole-forbidden. However, for a wide range of uranyl salts, these lowest energy transitions are observed, starting at energies just above 20 000 cm^{-1}. High-level theoretical calculations have been used to facilitate the interpretation of the crystal spectra and to explore the correlations between the states of UO2+2 in lattice environments and those of the free ion.[1,3−5,13−15]

Moving away from the high-symmetry environments of crystalline salts, Görller-Walrand et al.[12] examined the absorption and emission spectra of uranyl chloride (UO_2Cl_2) dissolved in polar nonaqueous solvents. They modified the local environment of the solvated UO2+2 ions by varying the Cl^- ion concentrations of their solutions. Other than having much broader features, the spectra for UO_2Cl_2 in solution were very similar to the results for crystalline $Cs_2UO_2Cl_4$. Changing the chloride ion concentration did not appear to shift the spectrum, which is consistent with the view that the external ligands are only weakly perturbing. However, the intensity distribution of the spectrum was dependent on the chloride ion concentration. Van Besien et al.[14] used CASPT2 calculations to examine the possibility that the concentration-dependent symmetry of the local solvation environment was responsible for the intensity changes. Their calculated transition energies were in reasonable agreement with experiment, but they were not able to reproduce the intensity data.

Gas-phase spectra for UO_2Cl_2 would be of value for further tests of the theoretical models, but such data have not been reported. In the present study, we have examined UO_2Cl_2 trapped in a solid Ar matrix. This minimally perturbing host provides data that can be compared with theoretical calculations for the isolated molecule.

Experimental Section

The matrix isolation unit used for this work has been previously described.[17] Samples of uranyl chloride in Ar were deposited on a CsI window that was cooled to a temperature of 12 K by a closed-cycle He refrigerator. Uranyl chloride was obtained by the hydrolysis of a sample of uranium tetrachloride. To obtain a useful vapor pressure, the sample was held in a Pyrex tube that was heated to ∼670 K using resistive heating tape. A slow flow of Ar through the heated tube was used to obtain the desired dilution ratio, and the gas mixture was deposited under effusive flow conditions. Typically, an Ar flow rate of 5 mmol/h was used, with a total deposition time of 3 h.

After deposition, the matrices were excited using the 308 nm light from a XeCl excimer laser or the tunable radiation from an excimer-pumped dye laser (Lambda Physik EMG 101/FL3002). Fluorescence from the matrix was collected by a collimating lens and focused through the entrance slits of a 0.64 m monochromator (ISA, 1200 lines/mm grating). In most experiments, long-pass filters were used to block laser scatter. Fluorescence was detected by a photomultiplier tube (Electron Tubes 9505QB).

Signals from the detector were processed by a digital oscilloscope (Tektronix TDS 1012) or boxcar integrator (SRS model 250). Both of these instruments were interfaced to a personal computer. Laser excitation and dispersed fluorescence

† Part of the "Russell M. Pitzer Festschrift".

* Corresponding author. E-mail: mheaven@emory.edu. Tel: (404) 727-6617. Fax: (404) 727-6586.

10.1021/jp9052133 CCC: $40.75
Published on Web 07/24/2009

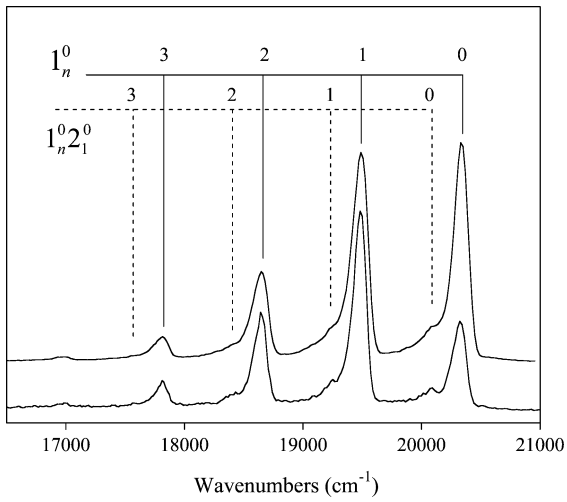

Figure 1. Dispersed fluorescence spectra for UO_2Cl_2 in solid Ar. The upper trace was obtained using 32 500 cm^{-1} excitation, whereas the lower trace was recorded using 22 669 cm^{-1} excitation.

spectra were recorded in this study. Time-gated fluorescence detection was used to minimize the interference from scattered laser light. For most of the spectra reported here, the fluorescence intensity was integrated over a 20 μs window that opened 15 μs after the laser pulse (nominally of 10 ns duration). Fluorescence decay curves were recorded using the signal-averaging capabilities of the digital oscilloscope.

The monochromator was calibrated using lines from a Hg emission lamp, and the wavelength scanning system of the dye laser was calibrated against a wavemeter (Bristol Instruments, model 821).

Results

Excitation of the Ar/UO_2Cl_2 matrices using photon energies above 20 350 cm^{-1} yielded a structured emission spectrum that spanned the range from 16 000 to 20 350 cm^{-1}. Figure 1 shows examples of dispersed fluorescence spectra. The upper trace was recorded using 32 500 cm^{-1} (308 nm) excitation, whereas the lower trace was obtained using dye laser excitation of an absorption band at 22 669 cm^{-1}. The intensity of the highest energy band in the lower trace has been reduced because a longer wavelength cutoff filter was used to reduce the laser scatter. Apart from this detail, the two spectra are essentially the same. Excitation of other bands in the 20 350−27 500 cm^{-1} range produced the same emission spectrum, indicating that rapid relaxation to the lowest-energy excited state occurred prior to fluorescence decay. The emission spectrum was dominated by a vibrational progression with a frequency of 840 cm^{-1}. In Figure 1, it can also be seen that each of the strong bands was accompanied by a weak shoulder that was red-shifted by approximately 240 cm^{-1}. The line width for the emission features (~130 cm^{-1} fwhm) was intrinsic to the sample. The transition energies for the emission bands, defined by their maximum intensity points, are listed in Table 1.

Laser excitation spectra were recorded using the detection of the fluorescence emitted at 19 481 cm^{-1}. Figure 2 shows the dye laser excitation range from 20 000 to 27 500 cm^{-1}. Note that several laser dyes were used to obtain this composite trace and that the band intensities have not been corrected for variations in the laser power. The gross intensity pattern is useful to consider, but small variations are not significant. The intensity of the peak at 24 303 cm^{-1} was artificially low because this was the crossover point between the ranges for the laser dyes

TABLE 1: Band Maxima and Band Spacings from the UO_2Cl_2 Emission Spectrum[a]

n	1_n^0	$1_n^0 2_1^0$
0	20 323	20 081
	(842)	(841)
1	19 481	19 240
	(839)	(840)
2	18 642	18 400
	(835)	
3	17 807	
	(835)	
4	16 972	

[a] Energies are given in inverse centimeters. The band maxima were determined to within ±5 cm^{-1}. The spacings between successive members of the stretch progressions are given as the values in parentheses in each column. Vibrational modes 1 and 2 are the UO_2^{2+} symmetric stretch and bending modes, respectively.

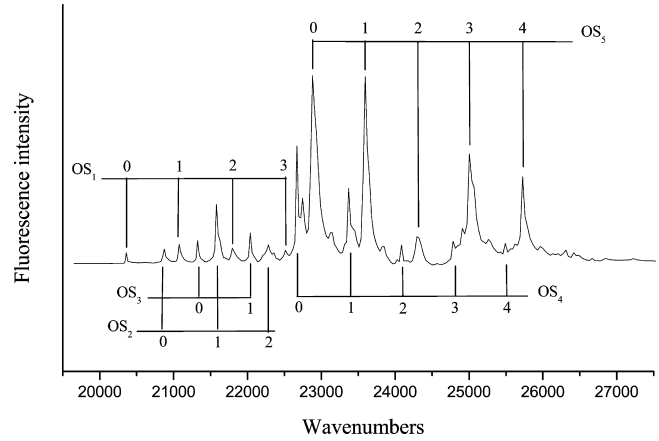

Figure 2. Laser-induced fluorescence spectrum for UO_2Cl_2 in solid Ar. This Figure was assembled from scans using a range of different laser dyes. The emission at 19 481 cm^{-1} was monitored.

TABLE 2: Band Maxima and Band Spacings from the UO_2Cl_2 Excitation Spectrum[a]

v_s	OS_1	OS_2	OS_3	OS_4	OS_5	$OS_5 + v_b = 1$
0	20 359	20875	21 325	22 669	22 881	23 140
	(717)	(706)	(713)	(709)	(713)	(712)
1	21 076	21581	22 038	23 378	23 594	23 852
	(720)	(702)	(710)	(705)	(709)	(708)
2	21 796	22283	22 748	24 083	24 303	24 560
	(718)		(710)	(706)	(709)	(700)
3	22 514		23 458	24 789	25 012	25 260
			(712)	(704)	(712)	(705)
4			24 170	25 493	25 724	25 965
				(707)	(696)	(702)
5				26 200	26 420	26 667

[a] Energies are given in inverse centimeters. The band maxima were determined to within ±2 cm^{-1}. The spacings between successive members of the stretch progressions are given as the values in parentheses in each column.

Stilbene 3 and PBBO. The linewidths observed in the excitation spectrum were also intrinsic to the sample, and in Figure 2, it can be seen that the linewidths varied for different absorption bands. The positions of the band maxima are listed in Table 2.

Fluorescence decay lifetimes were recorded using the excitation of most of the strong bands of Figure 2. The decay curves were not dependent on the feature initially excited, and a typical example is presented in Figure 3. The curves were clearly multiexponential and could be reasonably well-represented by a biexponential function of the form

$$I(t) = A_1 e^{-t/\tau_1} + A_2 e^{-t/\tau_2} \quad (1)$$

Nonlinear least-squares fitting yielded lifetimes of $\tau_1 = 50 \pm 5$ μs and $\tau_2 = 260 \pm 20$ μs for the fast and slow decay components. The ratio of the pre-exponential coefficients was $A_1/A_2 = 4.2$.

Following the observation of biexponential decays, we examined the dependence of the spectra on the segment of the decay curve used to determine the fluorescence intensity. We made a series of measurements using a gate delay of 30 μs and an integration window of 300 μs. The excitation and emission spectra obtained with these settings showed no discernible differences from those obtained using a gate delay of 20 μs and a 15 μs window. On the basis of the parameters obtained from fitting the decay curves, the spectra recorded with the 15 μs gate delay and 20 μs window reflected a 90% contribution from the short-lived component of the fluorescence, and this contribution was reduced to 40% for the data obtained with a 30 μs delay and 300 μs window.

Analysis and Discussion. The spectra for UO_2Cl_2 in Ar are closely similar to those of the crystalline uranyl salts[1,6,7,11] and UO_2Cl_2 in solution.[12] The band at 20 359 cm^{-1} in the excitation spectrum is readily identified as the origin of the lowest energy transition. This band is observed at 20 323 cm^{-1} in the emission spectrum, where the difference in the absorption and emission line maxima is due to the simultaneous excitation of Ar lattice phonons. This effect is often seen in the electronic spectra for molecules isolated in rare gas matrices. It indicates that electronic excitation causes a change in the guest−host interaction potential. (See, for example, ref 18.) For comparison, the lowest energy transition in absorption is observed at 20 096 cm^{-1} for $Cs_2UO_2Cl_2$[6] and 20 220 cm^{-1} for UO_2Cl_2 dissolved in tributylphosphate.[12]

The dominant progression of the emission spectrum (Figure 1) is the UO2+2 symmetric stretch, which has a vibrational frequency of 840 cm^{-1}. Again, this is close to the values observed for $Cs_2UO_2Cl_4$ (832 cm^{-1})[6] and solvated UO_2Cl_2 (~830 cm^{-1}).[12,19] The weak shoulder in the matrix spectrum, which defines a vibrational frequency of 240 cm^{-1}, is attributed to the UO2+2 bending modes. Calculations and previous spectroscopic studies indicate that there should be two modes with frequencies that are close enough that they would not be resolved in our spectra. For example, Flint and Tanner[20] observed bending frequencies of 238 and 249 cm^{-1} in the luminescence spectrum of $Cs_2UO_2Cl_4$.

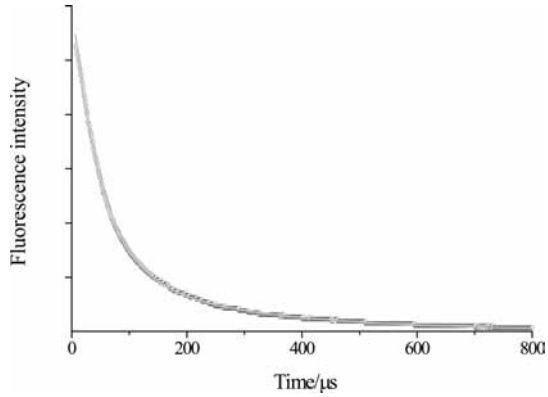

Figure 3. Fluorescence decay curve for UO_2Cl_2 in solid Ar. This trace was recorded using excitation at 20 359 cm^{-1} and detection at 19 481 cm^{-1}. The open circles represent the data points. The gray line is a biexponential fit to the data.

TABLE 3: Correlations between the Electronic States of UO_2Cl_2 in $D_{\infty h}$ and C_{2v} Symmetry

spin-free state, $D_{\infty h}$	spin−orbit coupled state (Ω), $D_{\infty h}$	states in C_{2v} symmetry
$^3\Delta_g$	1_g	$A_2 + B_1$
$^3\Delta_g$	2_g	$A_1 + B_2$
$^3\Delta_g$	3_g	$A_2 + B_1$
$^3\Phi_g$	2_g	$A_1 + B_2$
$^3\Phi_g$	3_g	$A_2 + B_1$
$^3\Phi_g$	4_g	$A_1 + B_2$
$^1\Delta_g$	2_g	$A_1 + B_2$
$^1\Phi_g$	3_g	$A_2 + B_1$

Relativistic density functional calculations[21] predict that the ground-state UO_2Cl_2 has a C_{2v} equilibrium structure with an O=U=O angle of 168° in the gas phase. The vibrational frequencies were predicted to be 848 cm^{-1} for the symmetric stretch and 182 cm^{-1} for the bend. Because the bending mode is soft, it is quite possible that part of the difference between the observed and calculated bending frequencies can be accounted for by guest−host interactions. For example, the bending frequency for neutral UO_2 in the gas phase is 121(±10) cm^{-1} (ref 22), but for UO_2 trapped in solid Ar, the frequency shifts to 225.2 cm^{-1} (ref 23). In this context, it should be noted that unusually large Ar matrix shifts have been observed for the antisymmetric stretch of UO_2[24,25] and the stretching modes of CUO.[26] These are open-shell species with low-lying electronically excited states. Andrews, Bursten, and coworkers[24,26−29] have proposed that large matrix shifts are observed because the guest−host interactions are strong enough to reorder the low-lying states. Such reordering will not be an issue for closed-shell UO_2Cl_2, where the first excited state is above 20 000 cm^{-1}. The increase in the bending frequency of UO_2Cl_2 (as compared with theory) is likely to be a simple consequence of the van der Waals repulsion between the O atoms and the surrounding lattice.

The excitation spectrum for UO_2Cl_2 in Ar had multiple progressions with vibrational spacings that were close to 710 cm^{-1} (cf. Table 2), the canonical UO2+2 symmetric stretch frequency for the first tier of excited states.[1] The gross pattern of band intensities indicates that each of the 710 cm^{-1} progressions belongs to a separate electronic state and that stretch progressions that are built on other vibrationally excited modes are not prominent in the spectrum. This interpretation is consistent with the analysis for $Cs_2UO_2Cl_4$, where the origins for seven electronic transitions were identified in the one-photon absorption spectrum below 27 800 cm^{-1} (ref 10). In the matrix spectrum, the strongest bands were observed for the fifth electronic transition, where weak features involving one quantum of the UO2+2 bending mode could be identified. The observed electronically excited states are labeled OS_1 to OS_5 in Table 2 and the following discussion.

It is well-established that the first tier of excited states is derived from the $\sigma_u\delta_u$ and $\sigma_u\phi_u$ configurations of UO2+2. Considered in terms of the properties of the linear ion,[1,3,4,14,15] these configurations give rise to the spin-free states $^3\Delta_g$, $^1\Delta_g$, $^3\Phi_g$, and $^1\Phi_g$. From these states, spin−orbit coupling gives rise to eight states that are characterized by the quantum number Ω, the unsigned projection of the electronic angular momentum along the molecular axis. Each state with $\Omega > 0$ is two-fold degenerate for the linear configuration, but this degeneracy is removed if the cylindrical symmetry is broken (e.g., reduced to C_{2v}). The correlation between states of $D_{\infty h}$ symmetry and those of C_{2v} symmetry is presented in Table 3. In C_{2v} symmetry,

TABLE 4: Comparison of Observed and Calculated Energies of Electronically Excited States of UO_2Cl_2

transition	upper state	E_{obsd}/cm^{-1} [a]	E_{calcd}/cm^{-1} [b]	osc. str./10^{-5} [c]
	$(1)1_g\ A_2$		20 338	
OS_1	$(1)1_g\ B_1$	20 359	20 375	0.0532
OS_2	$(1)2_g\ A_1$	20 875	20 771	0.0324
OS_3	$(1)2_g\ B_2$	21 325	20 979	0.0444
	$(1)3_g\ B_1$		21 844	
	$(1)3_g\ A_2$		21 900	
OS_4	$(2)2_g\ B_2$	22 669	23 201	5.792
OS_5	$(2)2_g\ A_1$	22 881	23 257	1.093

[a] UO_2Cl_2 in solid Ar (present work). [b] Calculated energies for $UO_2Cl_2(acetone)_3$ (C_{2v} geometry) from Table 4 of ref 14. [c] Calculated oscillator strengths for $UO_2Cl_2(acetone)_3$ (C_{2v} geometry) from Table 4 of ref 14.

the dipole selection rules permit transitions from the A_1 ground state to states of A_1, B_1, and B_2 character.

Assignments for the transitions observed in the matrix spectrum are proposed on the basis of comparisons with previous theoretical studies. In particular, the calculations of van Besien et al.[14] for solvated UO2+2 in C_{2v} coordination environments provide useful insight. The upper level for the OS_1 transition is consistently predicted to be the B_1 state that correlates with $\Omega = 1_g$ in the linear ion limit. The calculations of van Besien et al.[14] indicate that this state has over 95% $^3\Delta_g$ character. OS_2 and OS_3 correlate with the $(1)2_g$ state of uranyl (for this notation, the number in parentheses gives the ordering for the states of a given symmetry in ascending energy.) Here the calculations of van Besien et al.[14] predict that the leading eigenvectors for these states are approximately 60% $^3\Delta_g$ and 39% $^3\Phi_g$. The energy ordering of the $(1)2_g$ A_1 and B_2 states is sensitive to the surrounding ligands, but it appears that the transition to the B_2 component has a greater oscillator strength. On this basis, we tentatively assign OS_2 and OS_3 to the A_1 and B_2 components, respectively.

The next higher energy states are predicted to be the A_2 and B_1 components of $(1)3_g$. A transition to the former is symmetry-forbidden, and calculations indicate a very low oscillator strength for the transition to the B_1 component. The matrix spectrum did not show features that were compatible with assignment to $(1)3_g\ B_1$. OS_4 and OS_5 are assigned to the components of $(2)2_g$. The eigenvectors for these states are primarily $^3\Phi_g$ and $^3\Delta_g$, but they also include >15% $^1\Delta_g$.[14] This contribution of singlet character enhances the oscillator strength such that the transitions to the $(2)2_g$ states are the most intense for the spectral region below 30 000 cm^{-1}. As for the $(1)2_g$ states, the energy ordering of the A_1 and B_2 components is dependent on the ligands. On the basis of the intensities, OS_4 and OS_5 are assigned to the A_1 and B_2 states, respectively.

Using the above assignment scheme, we compare the observed electronic state energies with the theoretical predictions of van Besien et al.[14] in Table 4. The calculated oscillator strengths for transitions from the electronic ground state are also included.

The fluorescence decay behavior of UO_2Cl_2 in Ar was consistent with the dipole-forbidden nature of the lowest energy transition, but the biexponential decay was unexpected. The long-lived component was similar to the luminescence lifetimes reported for uranyl fluoride in solution. Beitz and Williams[30] reported a lifetime of 296 μs. If we assume that the long-lived component of the decay observed for UO_2Cl_2 represents the radiative lifetime (260 μs), then the oscillator strength is 1.4×10^{-5}. This is approximately one order of magnitude greater than the values computed by van Besien et al.[14] Given the difficulties involved in calculating small oscillator strengths, this level of disagreement is not of great concern. It is also possible that the observed lifetime is influenced by nonradiative relaxation to the ground state. The fast component of the decay gives an indication that such channels may be open. The observation that the fluorescence decay characteristics are independent of the initially excited state shows that the fast component of the decay is not related to processes whereby the excited molecule relaxes to the fluorescing state. A plausible explanation for the two-component decay is that it is related to a matrix site effect, where one type of site promotes nonradiative relaxation more rapidly than another. With this interpretation, the observation that the spectra were not sensitive to the temporal segment of the fluorescence that was integrated indicates that the line splitting caused by the presence of two trapping sites was small compared with the intrinsic widths of the vibronic bands.

Conclusions

Spectra for UO_2Cl_2 in solid Ar were recorded to obtain data that would approximate the characteristics of the unperturbed molecule. The results were consistent with the assignment of the lowest-energy electronic band systems to partially forbidden transitions of the UO2+2 moiety. The close similarity among the matrix data, the spectrum of crystalline $Cs_2UO_2Cl_4$, and the spectra for UO_2Cl_2 in nonaqueous solvents further supports the view that UO_2Cl_2 is not strongly perturbed by surrounding ligands. Five electronically excited states were identified in the matrix spectrum, and the energies of these states were in agreement with the theoretical predictions of van Besien et al.[14] The latter were carried out at the CASSCF/CASPT2 level of theory for UO2+2 with various coordinated ligands. It seems likely that calculations at this level or higher (e.g., relativistic coupled cluster methods[31]) for isolated UO_2Cl_2 would yield near-quantitative agreement with the present matrix results.

Acknowledgment. We gratefully acknowledge helpful discussions with Dr. Norman Edelstein (LBNL). Support for this work provided by the U.S. Department of Energy under grant DE-FG02-01ER15153-A005.

References and Notes

(1) Zhang, Z.; Pitzer, R. M. *J. Phys. Chem. A* **1999**, *103*, 6880.
(2) de Jong, W. A.; Visscher, L.; Nieuwpoort, W. C. *THEOCHEM* **1999**, *458*, 41.
(3) Wang, Q.; Pitzer, R. M. *J. Phys. Chem. A* **2001**, *105*, 8370.
(4) Matsika, S.; Zhang, Z.; Brozell, S. R.; Blaudeau, J. P.; Wang, Q.; Pitzer, R. M. *J. Phys. Chem. A* **2001**, *105*, 3825.
(5) Matsika, S.; Pitzer, R. M. *J. Phys. Chem. A* **2001**, *105*, 637.
(6) Denning, R. G. *J. Phys. Chem. A* **2007**, *111*, 4125.
(7) Denning, R. G. *Struct. Bonding (Berlin, Ger.)* **1992**, *79*, 215.
(8) Barker, T. J.; Denning, R. G.; Thorne, J. R. G. *Inorg. Chem.* **1992**, *31*, 1344.
(9) Denning, R. G.; Morrison, I. D. *Chem. Phys. Lett.* **1991**, *180*, 101.
(10) Barker, T. J.; Denning, R. G.; Thorne, J. R. G. *Inorg. Chem.* **1987**, *26*, 1721.
(11) Krupa, J. C.; Simoni, E.; Sytsma, J.; Edelstein, N. *J. Alloys Compd.* **1994**, *213*, 471.
(12) Goerller-Walrand, C.; De Houwer, S.; Fluyt, L.; Binnemans, K. *Phys. Chem. Chem. Phys.* **2004**, *6*, 3292.
(13) Pierloot, K.; van Besien, E.; van Lenthe, E.; Baerends, E. J. *J. Chem. Phys.* **2007**, *126*, 194311/1.
(14) van Besien, E.; Pierloot, K.; Goerller-Walrand, C. *Phys. Chem. Chem. Phys.* **2006**, *8*, 4311.
(15) Pierloot, K.; van Besien, E. *J. Chem. Phys.* **2005**, *123*, 204309/1.
(16) Nockemann, P.; Servaes, K.; Van Deun, R.; Van Hecke, K.; Van Meervelt, L.; Binnemans, K.; Goerller-Walrand, C. *Inorg. Chem.* **2007**, *46*, 11335.

(17) Nicolai, J. P.; Heaven, M. C. *J. Chem. Phys.* **1987**, *87*, 3304.
(18) Goodman, J.; Brus, L. E. *J. Chem. Phys.* **1977**, *67*, 4858.
(19) Soga, T.; Ohwada, K. *Spectrochim. Acta, Part A* **1999**, *55A*, 1337.
(20) Flint, C. D.; Tanner, P. A. *J. Chem. Soc., Faraday Trans. 2.* **1978**, *74*, 2210.
(21) Kovacs, A.; Konings, R. J. M. *THEOCHEM* **2004**, *684*, 35.
(22) Han, J.; Goncharov, V.; Kaledin, L. A.; Komissarov, A. V.; Heaven, M. C. *J. Chem. Phys.* **2004**, *120*, 5155.
(23) Green, D. W.; Reedy, G. T.; Gabelnick, S. D. *J. Chem. Phys.* **1980**, *73*, 4207.
(24) Zhou, M.; Andrews, L.; Ismail, N.; Marsden, C. *J. Phys. Chem. A* **2000**, *104*, 5495.
(25) Hunt, R. D.; Andrews, L. *J. Chem. Phys.* **1993**, *98*, 3690.
(26) Li, J.; Bursten, B. E.; Liang, B.; Andrews, L. *Science* **2002**, *295*, 2242.
(27) Andrews, L.; Liang, B.; Li, J.; Bursten, B. *Angew. Chem., Int. Ed.* **2000**, *39*, 4565.
(28) Andrews, L.; Liang, B.; Li, J.; Bursten, B. E. *J. Am. Chem. Soc.* **2003**, *125*, 3126.
(29) Li, J.; Bursten, B. E.; Andrews, L.; Marsden, C. J. *J. Am. Chem. Soc.* **2004**, *126*, 3424.
(30) Beitz, J. V.; Williams, C. W. *J. Alloys Compd.* **1997**, *250*, 375.
(31) Infante, I.; Eliav, E.; Vikas, M. J.; Ishikawa, Y.; Kaldor, U.; Visscher, L. *J. Chem. Phys.* **2007**, *127*, 124308.

JP9052133